Cell Metabolism
Article

Translational Control of Mitochondrial Energy Production Mediates Neuron Morphogenesis

Aparna Oruganty-Das,[1] Teclise Ng,[2] Tsuyoshi Udagawa,[1,3] Eyleen L.K. Goh,[2] and Joel D. Richter[1,*]
[1]Program in Molecular Medicine, University of Massachusetts Medical School, Worcester, MA 01605, USA
[2]Program in Neuroscience and Behavioral Disorders, Duke-NUS Graduate Medical School, Singapore 169857, Singapore
[3]Present address: Department of Neurology, Nagoya University, 65 Tsurumai-cho, Showa-ku, Nagoya-shi, Aichi 466-8550, Japan
*Correspondence: joel.richter@umassmed.edu
http://dx.doi.org/10.1016/j.cmet.2012.11.002

SUMMARY

Mitochondrial energy production is a tightly regulated process involving the coordinated transcription of several genes, catalysis of a plethora of posttranslational modifications, and the formation of very large molecular supercomplexes. The regulation of mitochondrial activity is particularly important for the brain, which is a high-energy-consuming organ that depends on oxidative phosphorylation to generate ATP. Here we show that brain mitochondrial ATP production is controlled by the cytoplasmic polyadenylation-induced translation of an mRNA encoding NDUFV2, a key mitochondrial protein. Knockout mice lacking the Cytoplasmic Polyadenylation Element Binding protein 1 (CPEB1) have brain-specific dysfunctional mitochondria and reduced ATP levels, which is due to defective polyadenylation-induced translation of electron transport chain complex I protein NDUFV2 mRNA. This reduced ATP results in defective dendrite morphogenesis of hippocampal neurons both in vitro and in vivo. These and other results demonstrate that CPEB1 control of mitochondrial activity is essential for normal brain development.

INTRODUCTION

Mitochondrial ATP production accounts for ~90% of the energy produced in mammalian cells, and thus the regulation of mitochondrial function is critically important for cell growth and viability. Nuclear-encoded mitochondrial proteins are regulated transcriptionally by various factors such as nuclear respiratory factors NRF1 and NRF2, stimulatory protein 1 (Sp1), estrogen-related receptor α (ERRα), and yin yang 1 transcription factor (YY1) (Scarpulla, 2008). PGC1α plays a role in coordinating the expression of mitochondrial subunits commensurate with changes in the environment (Lin et al., 2005). Mitochondrial activity is also regulated by the formation of supercomplexes that allow for substrate channeling (Shoubridge, 2012). Post-translational modifications affect mitochondrial function (Koc and Koc, 2012), as does tissue-specific expression of different mitochondrial proteins that generate unique mitochondrial dynamics to accommodate different requirements for a given tissue (Pagliarini et al., 2008).

The cytoplasmic polyadenylation element binding proteins (CPEBs) are a family of four RNA binding proteins that are widely expressed in vertebrates (Mendez and Richter 2001). CPEB1 is the founding member of this family; it associates with the cytoplasmic polyadenylation element (CPE), a U-rich (UUUUUAU) structure generally residing within 100 bases of the AAUAAA pre-mRNA cleavage and polyadenylation signal in the 3′UTRs of specific mRNAs. CPEB proteins 2–4 probably also associate with U-rich structures (Novoa et al., 2010), but they do not appear to recognize the CPE with the same high affinity as CPEB1 (Huang et al., 2006). Although all CPEB proteins regulate mRNA expression (Huang et al., 2006; Chen and Huang 2011; Novoa et al., 2010; Wang and Huang 2012), CPEB1 is centrally important for promoting translation by stimulating cytoplasmic polyadenylation. CPEB1 is the key component of the cytoplasmic polyadenylation complex, which also includes cleavage and polyadenylation specificity factor (CPSF), the noncanonical poly(A) polymerase Gld2, the deadenylating enzyme PARN, the scaffold protein symplekin, poly(A) binding protein (PABP), and Maskin or Neuroguidin (Ngd), which also bind the cap-binding factor eIF4E (Barnard et al., 2004; Kim and Richter 2006, 2007; Richter 2007; Udagawa et al., 2012). When associated with these factors in a large ribonucleoprotein (RNP) complex, CPE-containing mRNAs have short poly(A) tails and are translationally repressed. In response to an environmental cue, the kinase Aurora A phosphorylates CPEB1, which causes the dissociation of PARN from the RNP complex, resulting in default Gld2-catalyzed polyadenylation (Mendez et al., 2000; Kim and Richter 2006). The newly elongated poly(A) tail then is bound by PABP, which also binds the initiation factor eIF4G. eIF4G subsequently displaces Maskin from eIF4E and thereby recruits other initiation factors and the 40S ribosomal subunit to the 5′ end of the mRNA (Cao et al., 2006; Kim and Richter 2007).

CPEB1-mediated translation is required for several biological phenomena including oocyte development (Tay and Richter 2001), neuronal synaptic plasticity and learning and memory (Alarcon et al., 2004; Berger-Sweeney et al., 2006; Zearfoss et al., 2008; Udagawa et al., 2012), cell growth (Groisman et al., 2006; Burns and Richter 2008), and hepatic insulin resistance (Alexandrov et al., 2012). Fibroblasts derived from CPEB1 knockout (KO) mice bypass senescence, as do human skin fibroblasts depleted of CPEB1 (Groisman et al., 2006; Burns and Richter 2008); in both cell types, reduced p53 mRNA translation is a key event causing the immortalization (Burns and

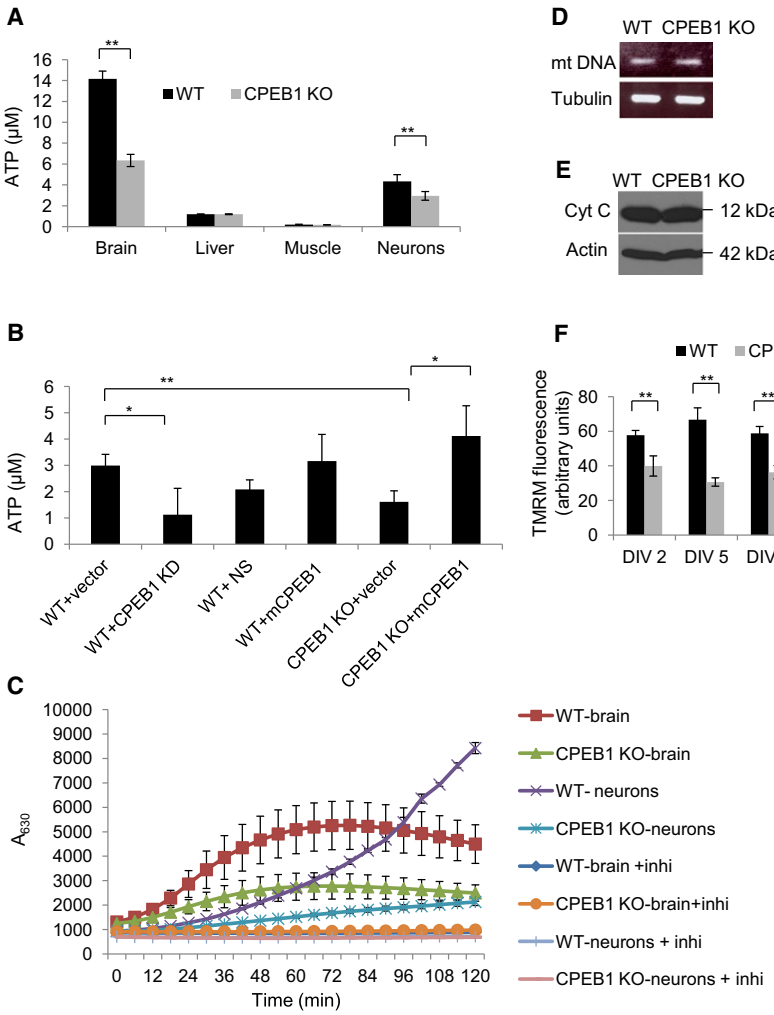

Figure 1. CPEB1 Controls Mitochondrial ATP Production

(A) ATP levels in brain, liver, muscle, and hippocampal neurons from five WT and five CPEB1 KO mice.

(B) ATP in WT and CPEB1 KO hippocampal neurons isolated from three different embryos infected with lentiviruses expressing shRNA against CPEB1 (CPEB1 KD), nonsilencing shRNA (NS), or HA-tagged CPEB1 (CPEB1).

(C) Oxygen consumption in four WT and four CPEB1 KO brain and cultured hippocampal neurons with or without the inhibitors (inhi) rotenone plus antimycin.

(D) Quasiquantitative PCR of mitochondrial (mt) and tubulin DNAs in WT and CPEB1 KO brain.

(E) Western blots of the mitochondrial protein cytochrome *c* and actin in WT and CPEB1 KO brain.

(F) Mitochondrial membrane potential as measured by TMRM in seven hippocampal neurons each from eight WT and eight CPEB1 KO embryos cultured for 2–20 DIV. *p < 0.05; **p < 0.01 Student's t test, all experiments were done in three replicates, the bars indicate SEM. See also Figure S1.

Richter 2008; Groppo and Richter 2011). CPEB1 depletion, at least in human fibroblasts, results in the Warburg effect, a cancer-related phenomenon in which ATP production by mitochondrial oxidative phosphorylation is impaired but compensated for by increased glycolysis (Burns and Richter 2008; Levine and Puzio-Kuter 2010; Vander Heiden et al., 2009). The reduced p53 levels in CPEB1-depleted cells lowers synthesis of cytochrome *c* oxidase (SCO2), which in turn impairs electron transport chain complex IV activity.

In this study, we sought to investigate whether CPEB1 deficiency results in impaired mitochondrial function in animal tissue. Surprisingly, we observed that in CPEB1 KO animals, mitochondrial energy production was reduced in the brain and neurons but not muscle or liver and was unaccompanied by elevated glycolysis as occurs in the Warburg effect. Further analysis showed that the polyadenylation of electron transport chain complex I protein NDUFV2 mRNA was compromised in neurons, which caused reduced levels of the protein and hence inefficient oxygen consumption and ATP production. As a consequence of depressed ATP levels, dendrite morphogenesis was also reduced in CPEB1-deficient hippocampal neurons both in vitro and in vivo. Impaired dendrite branching and growth in CPEB1-deficient neurons was rescued when normal levels of ATP were restored. These and other observations reveal an essential and unexpected role for translational control in energy production in the brain.

RESULTS

CPEB1 Deficiency Leads to Reduced Mitochondrial Function

To assess whether CPEB1 KO mice have altered bioenergetics similar to CPEB1-depleted fibroblasts, ATP levels were measured in extracts from brain, liver, and muscle. Although the latter two tissues had no change in ATP concentration compared to wild-type (WT), the brain displayed an ~56% reduction, while cultured hippocampal neurons derived from CPEB1 KO mice showed a 32% reduction (Figure 1A). We measured the recovery of ATP from brain lysates by titrating in known amounts of this nucleoside triphosphate. Using our extraction procedure, there was a 41% recovery of ATP from WT and a 50% recovery from CPEB1 KO brain lysates; consequently, the values shown in the figure reflect corrected values for the recovery of ATP. The reduced ATP in CPEB1 KO brain may be contrasted to the effect observed in human foreskin fibroblasts in which CPEB1 depletion, while reducing mitochondrial ATP production, had no effect on overall ATP levels because of a compensatory upregulation of glycolysis. This phenomenon of reduced mitochondrial ATP production and elevated glycolysis is known as the Warburg effect and is a characteristic of cancer cells that may contribute to malignant transformation (Vander Heiden et al., 2009; Dang, 2012). In the brain, normal levels of ATP were restored in the CPEB1 KO neurons when they were infected with lentivirus expressing CPEB1-HA (Figure 1B), indicating that the depletion

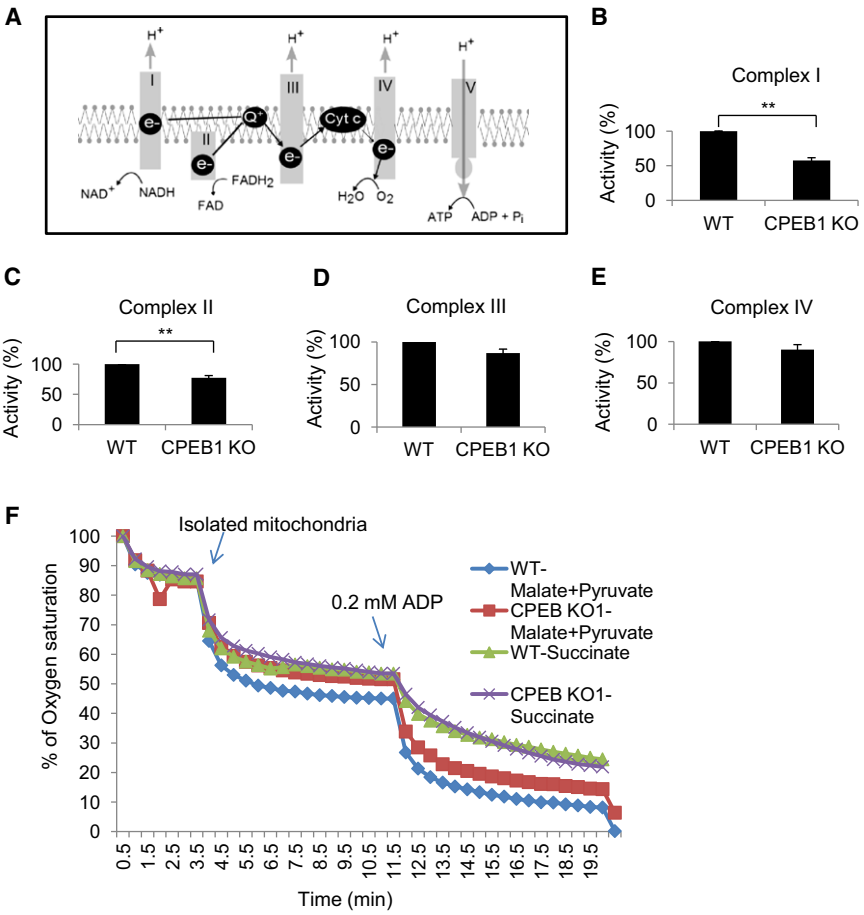

Figure 2. CPEB1 Regulates the Activity of Electron Transport Chain Complex I

(A) Schematic of mitochondrial electron transport chain complexes I–V.

(B–E) Activities of electron transport chain (ETC) complexes I-IV in mitochondria from three WT and three CPEB1 KO mouse brain.

(F) Oxygen consumption of mitochondria isolated from WT or CPEB1 KO brains. Mitochondria were incubated in a chamber containing an oxygen sensor; oxygen consumption was measured in the presence of complex I (malate plus glutamate) or complex II substrates (succinate). ADP was added to stimulate state 3 respiration. *$p < 0.05$; **$p < 0.01$ Student's t test, three replicates, the bars indicate SEM. See also Figure S2 and Table S1.

of ATP is reversible. Next, we determined whether shRNA depletion of CPEB1 in WT neurons had a similar effect on ATP generation. As shown in Figure S1A (available online), an ~65% depletion of CPEB1 was accompanied by an ~65% reduction in ATP only upon shRNA depletion of this protein, but not when a control nonsilencing (NS) shRNA was used (Figure 1B). These results show that CPEB1 controls energy balance specifically in neurons.

To investigate how CPEB1 regulates ATP levels, oxygen consumption was measured and shown to be reduced by ~50% in CPEB1 KO brain as well as cultured CPEB1 KO hippocampal (Figure 1C) and cortical neurons (Figure S1B); oxygen consumption in CPEB1 KO glia, however, was unchanged (Figure S1C). Oxygen consumption in brain lysates and hippocampal neurons was also determined in the presence of mitochondrial inhibitors rotenone plus antimycin and shown to be completely inhibited, indicating that the oxygen consumption we measured was entirely mitochondrial (Figure 1C). We also found that oxygen consumption in brain lysates increased for 54 min, after which time it diminished. This nonlinear measurement could be due to clumps of cells in the brain lysates that might have incomplete access to nutrients and oxygen, thus leading to the death of some of the neurons. Lactate production, which indicates efficiency of glycolysis, was unaltered in CPEB1 KO brain or neurons (Figure S1D), demonstrating that the reduction in ATP was not compensated by enhanced glycolysis.

Mitochondrial levels as determined by mitochondrial DNA (Figure 1D) and cytochrome *c* content (Figure 1E) were unchanged in neurons, indicating that an alteration in the mass of mitochondria was not responsible for reduced ATP production in CPEB1-depleted neurons. Mitochondrial morphology in WT and CPEB1 KO neurons as determined by confocal microscopic examination of mitotracker-stained cells showed no significant differences (Figure S1E), indicating that the gross morphology of mitochondria was unaffected by the loss of CPEB1. However, mitochondrial membrane potential as measured by the fluorescent dye tetramethylrhodamine methyl ester (TMRM) was reduced by 40%–60% in DIV 2-20 cultured CPEB1 KO neurons (Figure 1F). These data demonstrate that mitochondrial function, but not mitochondrial mass, is reduced in CPEB1 KO brain and neurons.

Mitochondrial Insufficiency Is Due to an Impairment of Electron Transport Chain Complex I

The electron transport chain consists of four multiprotein complexes that sequentially transfer electrons to generate a proton gradient across the inner mitochondrial membrane, which is utilized by ATP synthase to phosphorylate ADP to produce ATP (Figure 2A). The actions of each of the complexes were measured in mitochondria isolated from WT and CPEB1 KO mouse brains. Because exogenous substrates were used for the assays, each complex was not influenced by the activity of any other. The activities of complexes I and II showed a statistically significant decline in the CPEB1 KO mitochondria; complex I activity in particular was strongly reduced by ~60% (Figures 2B–2E). Citrate synthase, which indicates mitochondrial function unrelated to electron transport, was similar in WT and CPEB1 KO brain (Figure S2A). Complex I and II activities were also determined by measuring oxygen consumption of isolated respiring mitochondria using an oxygen electrode. Oxygen consumption was measured in the presence of complex I substrates malate plus glutamate or succinate, a complex II substrate. As

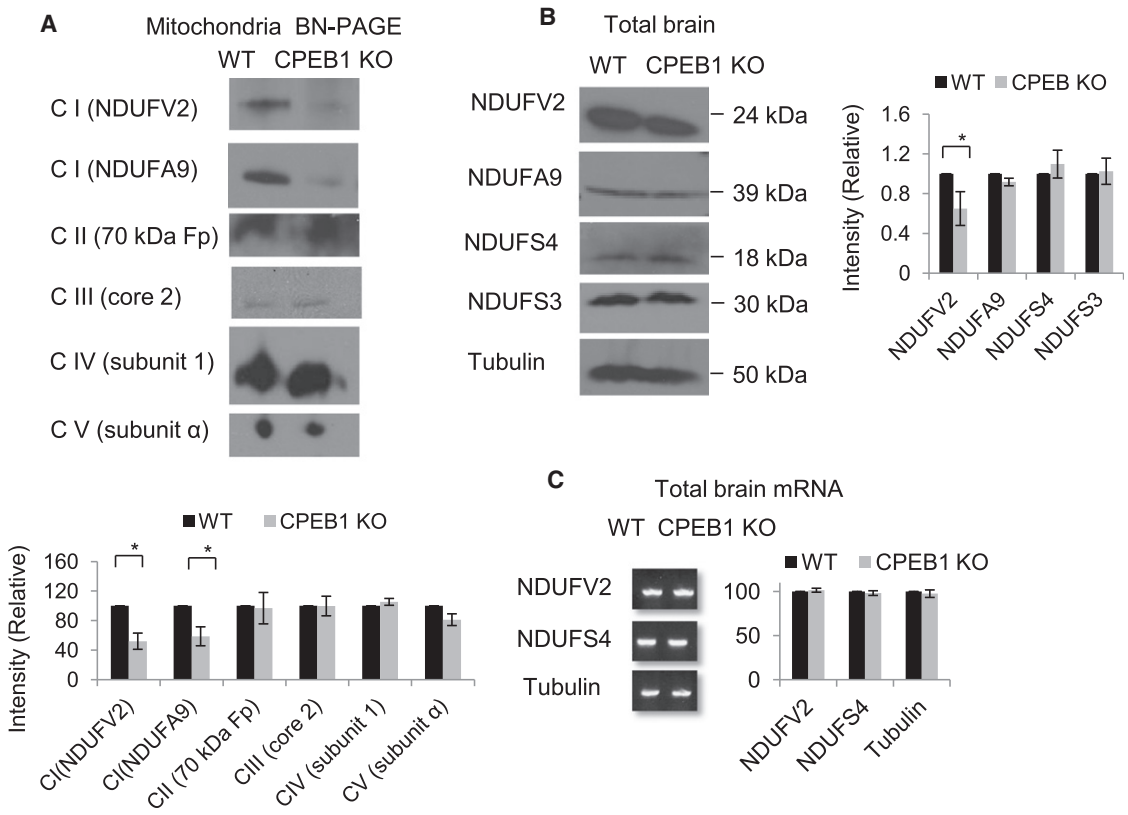

Figure 3. CPEB1 Regulates the Expression of Complex I Protein NDUFV2

(A) Blue native PAGE-resolved intact ETC complexes from mitochondria isolated from three WT and three CPEB1 KO brains and selected proteins in complexes I–V were analyzed by western blotting. Quantification is shown on the histogram.

(B) Western blots were probed for mitochondrial proteins from total lysates from three WT and three CPEB1 KO brains. Quantification is shown on the histogram.

(C) Quantitative RT-PCR analysis of NDUFV2, NDUFS4, and tubulin mRNAs in three WT and three CPEB1 KO brains. *$p < 0.05$; **$p < 0.01$ Student's t test, three replicates, the bars indicate SEM.

shown in Figure 2F and Table S1, oxygen consumption in both WT and CPEB1 KO mitochondria increased significantly upon addition of mitochondria to the reaction mix. The rate of oxygen consumption further increased upon addition of ADP (state 3 respiration). However, the rate of oxygen consumption was lower in CPEB1 KO mitochondria in the presence of complex I substrates but was unaffected in the presence of the complex II substrate, again demonstrating that CPEB1 KO mitochondria are defective for complex I activity.

Reactive oxygen species (ROS) were increased by ~60 and 80% in the CPEB1 KO brain and neurons, respectively (Figure S2B). Complex I is a significant generator of ROS in mitochondria, which could explain why CPEB1 KO mitochondria have increased ROS. To determine whether the increased ROS leads to increased oxidative damage, the levels of protein carbonyl groups were measured as an indicator of oxidative damage. Carbonyl groups are produced on amino side chains (especially of proline, arginine, lysine, and threonine) when they are oxidized. As shown in Figure S2C, CPEB1 KO brain had only very slightly elevated protein oxidative damage.

We next used blue native PAGE and western blotting to examine specific proteins in each intact complex isolated from WT and CPEB1 KO mitochondria. Because the blue native PAGE is nondenaturing, the electron transport chain complexes remain intact and are not dissociated into their constituent subunits. Figure 3A shows that in contrast to proteins in complexes II, III, IV, and V, complex I was reduced by ~40% (as shown by blotting for its proteins NDUFV2 and NDUFA9) in the CPEB1 KO mitochondria. Complex II was not affected in the blue native PAGE analysis, but its activity was reduced by about 20% in CPEB1 KO mitochondria (Figure 2C), suggesting that the dysfunction in complex II is not due to the loss of its constituent proteins. Examination of complex I proteins in total brain extracts demonstrates a reduction, by ~35%, only of NDUFV2 in the CPEB1 KO samples (Figure 3B). NDUFV2 mRNA levels, however, were comparable in WT and CPEB1 KO brain (Figure 3C). These data suggest not only that reduced NDUFV2 in CPEB1 KO mitochondria is responsible for impaired ATP production but that the levels of this protein might also be regulated at the posttranscriptional level.

Complex I Protein NDUFV2 Expression Is Reduced in CPEB1 KO Mice

NDUFV2 is one of 14 core catalytic subunits of complex I; it is synthesized in the cytoplasm and imported into mitochondria via an amino-terminal mitochondrial targeting sequence (MTS) (Figure 4A). To test whether reduced NDUFV2 in CPEB1 KO mitochondria is responsible for impaired ATP production,

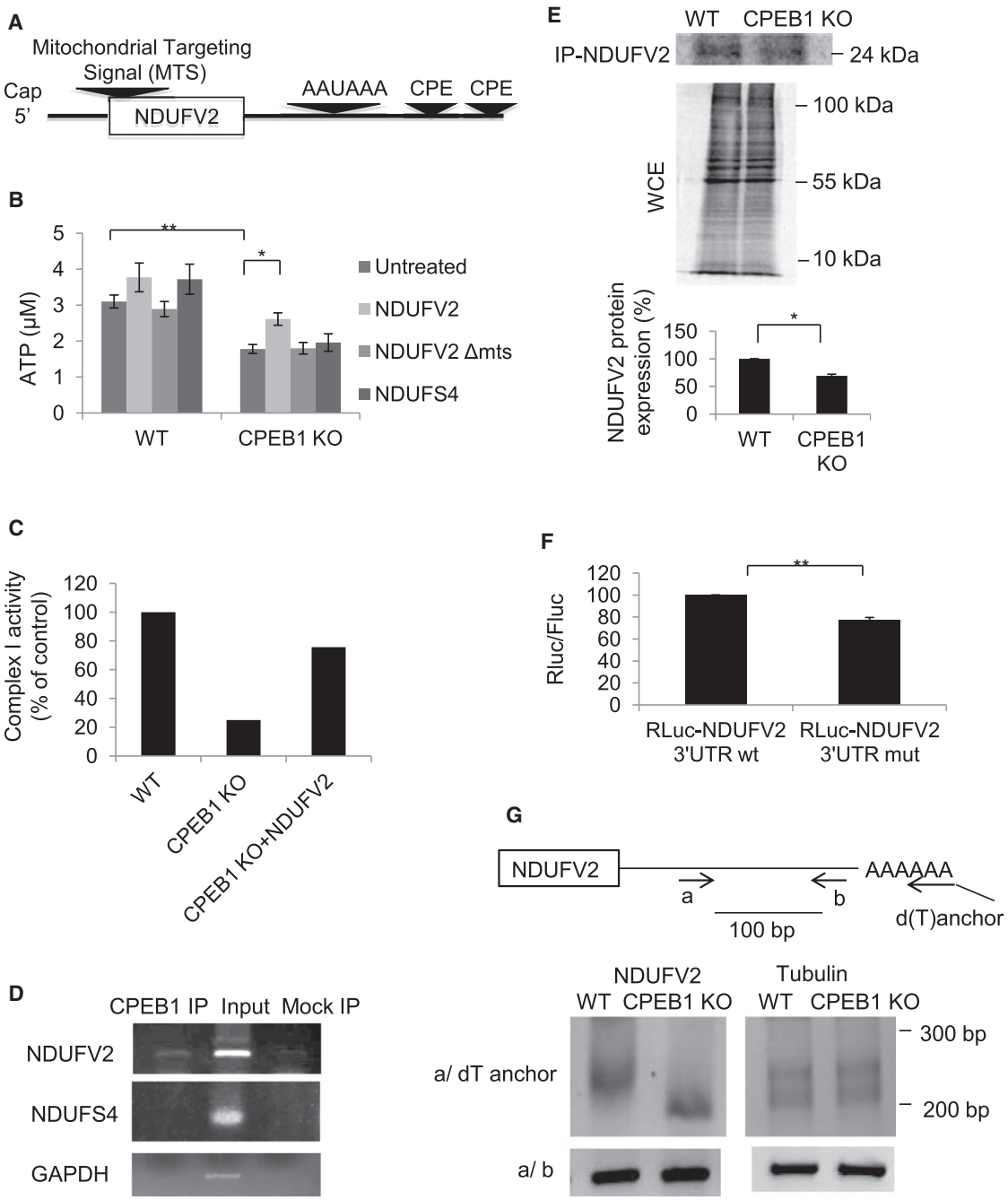

Figure 4. CPEB1 Regulates NDUFV2 mRNA Translation

(A) Schematic of NDUFV2 mRNA showing the mitochondrial targeting signal, polyadenylation hexanucleotide AAUAAA, and CPEs.

(B) ATP was measured in WT and CPEB1 KO hippocampal neurons infected with lentiviruses expressing NDUFV2, or a mutant NDUFV2 lacking the MTS or NDUFS4.

(C) Complex I activity was measured in WT and CPEB1 KO hippocampal neurons infected with lentivirus expressing NDUFV2.

(D) WT hippocampal neurons were infected with lentivirus expressing HA-CPEB1. HA antibody was used to coimmunoprecipitate CPEB1 followed by RT-PCR for NDUFV2, NDUFS4, and GAPDH mRNAs.

(E) WT and CPEB1 KO hippocampal neurons were incubated with ^{35}S-methionine followed by immunoprecipitation of NDUFV2 and analysis by SDS-PAGE. WCE refers to whole cell extract. The histogram shows the quantification of immunoprecipitation.

(F) The coding region of Renilla luciferase was appended with the WT NDUFV2 3′UTR or one that lacked the CPEs (3′UTR mut) (see A). Plasmids encoding these constructs as well as firefly luciferase to serve as a control were transfected into neurons and analyzed for luciferase activity 3 days later. The data are plotted as the ratio of Renilla luciferase activity to firefly luciferase activity.

(G) A PCR-based polyadenylation assay was used to determine the poly(A) tails of NDUFV2 and tubulin mRNAs in WT and CPEB1 KO brain (primers a/dT anchor). The internal primers (a/b) indicate the relative amount of RNA in each sample. *$p < 0.05$; **$p < 0.01$ Student's t test, three replicates, the bars indicate SEM.

CPEB1 KO neurons were infected with lentiviruses expressing NDUFV2, or as controls, NDUFV2 that lacks a MTS or NDUFS4. Figure 4B shows that ATP levels were restored to nearly WT levels by ectopic MTS-containing, but not MTS-lacking, NDUFV2. ATP levels were unaffected by ectopic expression of NDUFS4 (a complex I constituent whose levels were unchanged in CPEB1 KO), suggesting that the effect on ATP in CPEB1 KO neurons is specifically due to reduced NDUFV2 (Figure 4B). Complex I activity in CPEB1 KO neurons was also restored to nearly WT levels by ectopic expression of NDUFV2 (Figure 4C). These results demonstrate that reduced NDUFV2 in CPEB1 KO neurons leads to deficient mitochondrial ATP production.

NDUFV2 mRNA contains 3′UTR CPEs, which although downstream of the AAUAAA could still support cytoplasmic polyadenylation (Fox et al., 1989). Based on this observation, we thought this mRNA might be directly regulated by CPEB1. To assess this possibility, WT neurons were infected with a lentivirus expressing CPEB1-HA, followed by HA immunoprecipitation and RT-PCR analysis for coprecipitating RNAs. As shown in Figure 4D, NDUFV2 mRNA was immunoprecipitated with CPEB1-HA, but not when the cells were not transduced with CPEB1-HA (mock IP). GAPDH and NDUFS4 mRNAs were not coprecipitated with CPEB1-HA, indicating its specificity for NDUFV2.

The decrease in amount of NDUFV2 in CPEB1 KO brains (Figure 3B) could be due to decreased translation or increased degradation. To determine whether the synthesis of NDUFV2 is altered in CPEB1 KO neurons, cells were pulse labeled with ^{35}S-methionine for 1 hr followed by immunoprecipitation with NDUFV2 antibody. Because of the short incubation time, the radiolabeled NDUFV2 reflects new synthesis but very little degradation because protein destruction usually occurs over several hours. Figure 4E shows that NDUFV2 was synthesized ~40% less efficiently in CPEB1 KO compared to WT neurons, suggesting that CPEB1 mediates the translation of NDUFV2 mRNA. To investigate this possibility further, neurons were transfected with plasmids encoding firefly luciferase mRNA (transfection control) and Renilla luciferase mRNA appended with the NDUFV2 3′UTR containing or lacking the CPEs (see Figure 4A). When determined 3 days after transfection, the Renilla luciferase activity was 25% higher when the reporter RNA contained the 3′UTR CPEs (Figure 4F). These data indicate that the CPEs promote the translation of NDUFV2 mRNA.

Finally, an examination of NDUFV2 mRNA shows that the length of its poly(A) tail was reduced by ~30 nt in CPEB1 KO versus WT brain; the poly(A) tail of tubulin mRNA was similar in each genotype (Figure 4G). Equal amounts of NDUFV2 and tubulin mRNAs from WT and CPEB1 KO were used for the assay. Taken together, the data in Figure 4 indicate that the control of ATP levels in neurons by CPEB1 is mediated by polyadenylation and translation of NDUFV2 mRNA.

Dendritic Branching Is Impaired in CPEB1 KO Mice

We surmised that reduced brain ATP in CPEB1 KO mice might impair neuron growth and/or morphogenesis. To assess this possibility, neurons from WT and CPEB1 KO mice were immunostained for tubulin and subjected to a Sholl analysis in which concentric rings surrounding a neuron with the cell body in the center are used to measure dendrite branching. Although neurons from both genotypes appeared similar during the initial days of culture, by day 5 (Figure 5A) the CPEB1 KO neurons showed 16% fewer dendrite branches (Figure 5B); dendrite length was also reduced by ~19% (Figure 5C). This result is similar to that observed by Bestman and Cline (2008), who examined the role of CPEB1 in dendrite morphogenesis using *Xenopus laevis* optic tectal neurons. Dendrite branching was restored when CPEB1 was ectopically expressed in the DIV5 CPEB1 KO neurons following lentivirus infection (Figures S3A and S3B). Moreover, reduced branching was observed in DIV5 WT neurons following shRNA-mediated CPEB1 depletion (Figures S3A and S3B). These data demonstrate that CPEB1 controls dendrite morphology.

To investigate whether reduced ATP production is causative for diminished dendrite arborization, CPEB1 KO neurons were cultured in medium containing phosphocreatine for 4 days in vitro (DIV), which increased ATP levels to nearly WT levels (Figure 5D) and dendrite branching to near WT levels (Figures 5E and 5F). Treatment of WT neurons with phosphocreatine, which donates a high-energy phosphate to ADP to produce ATP, enhanced dendrite branching (Figures 5E and 5F). These results indicate that inhibited dendrite development in CPEB1 KO neurons is most likely due to impaired ATP generation.

To examine whether CPEB1 regulates dendrite extension in vivo, retroviruses expressing GFP and a scrambled or CPEB1-directed shRNA were injected into the dentate gyrus (DGs) of 6- to 7-week-old mice (Ge et al., 2006). Two weeks post-injection, the dividing DG neurons were analyzed by serial sectioning and three-dimensional reconstruction of confocal images of GFP-immunostained cells. Total dendrite length and branching were reduced by more than 50% in the knockdown (KD) compared to WT neurons (Figures 6A–6C). CPEB1 depletion also reduced dendritic branching complexity of the neurons (Figure 6D). Injection of a second shRNA against CPEB1 resulted in similar deficits in dendrite length and branching (data not shown). Taken together, these data demonstrate that CPEB1 mediates neuronal maturation in vitro and in vivo.

To assess whether ectopic expression of NDUFV2 in neurons rescues the reduction in dendrite morphology by CPEB1 depletion in vivo, retroviruses expressing CPEB1 shRNA and NDUFV2 containing or lacking its MTS were injected into the DG as was performed previously, followed by serial sectioning and 3D reconstruction of GFP-stained images. Figures 6E and 6F show that dendrite branch number as well as dendritic length were increased upon expression of NDUFV2 containing but not lacking its MTS. The dendrite branching defect was also rescued by ectopic expression of NDUFV2, but not NDUFS4 in CPEB1 KO neurons in culture (Figure 6G), thus reaffirming the importance of NDUFV2 and mitochondrial energy production in dendrite branching.

Figure 7 shows a model that summarizes the data described above. In WT neurons, CPEB1 is associated with the 3′UTR CPEs of NDUFV2 mRNA. At steady state or perhaps in response to an environmental cue, CPEB1 promotes poly(A) tail growth and translation of the mRNA, resulting in NDUFV2 protein import into the inner mitochondrial membrane, where it is incorporated into complex I, thereby increasing flow of electrons through the electron transport chain, and finally ATP is generated. When neurons are CPEB1 deficient, reduced NDUFV2 mRNA translation

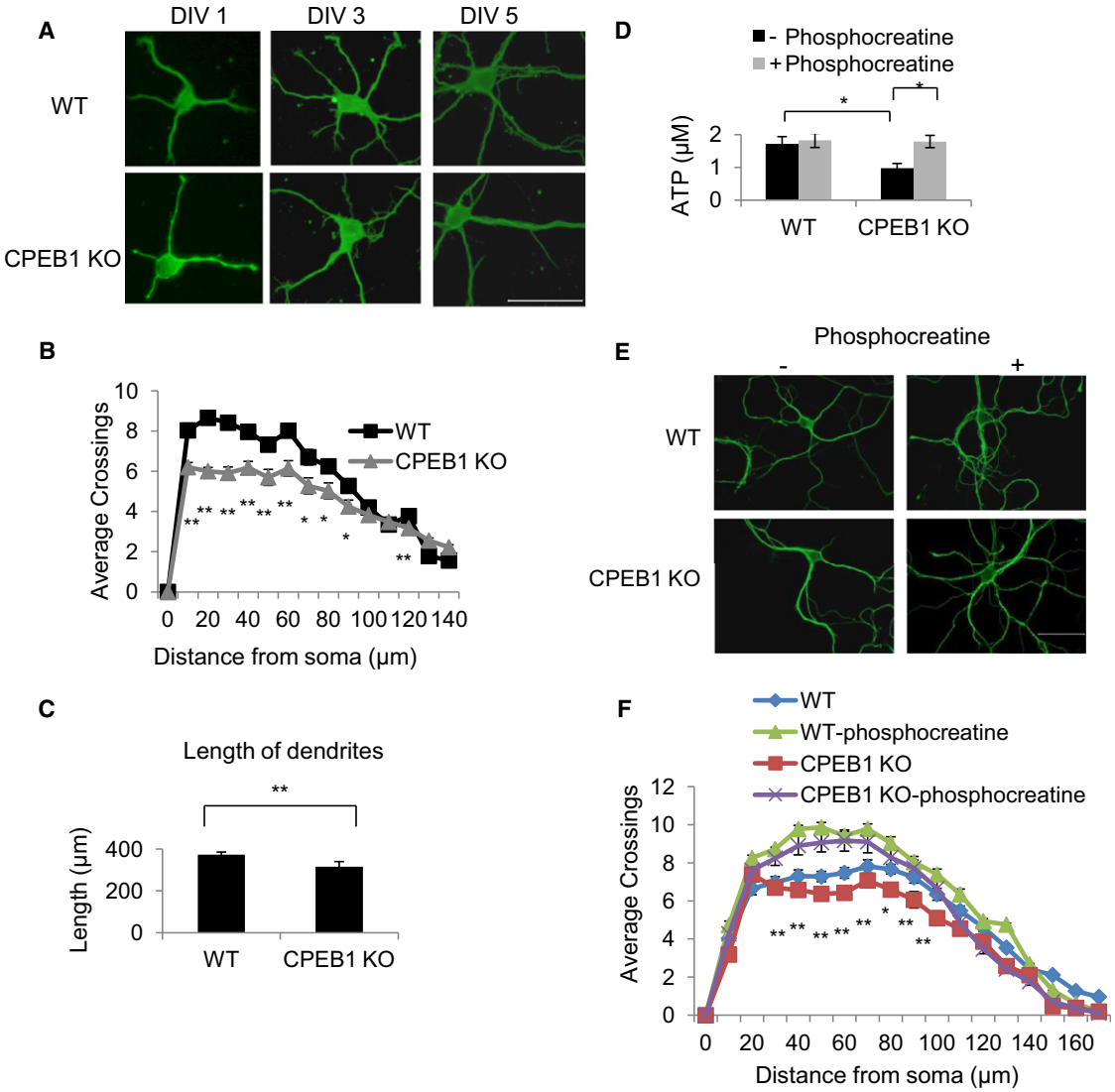

Figure 5. CPEB1 and ATP Promote Dendritic Development

(A) Morphology of WT and CPEB1 KO hippocampal neurons immunostained for tubulin at different days of culture. Scale bar, 50 μm.

(B) Sholl analysis was performed on WT and CPEB1 KO neurons cultured for 5 days (n = 60 neurons from three mice).

(C) Dendrite length was determined for cultured WT and CPEB1 KO neurons (n = 50 dendrites of 14 neurons from three mice).

(D) WT and CPEB1 KO neurons were continuously supplemented with phosphocreatine followed by determination of ATP at DIV6.

(E) Morphology of DIV6 WT and CPEB1 KO neurons following treatment with phosphocreatine; they were immunostained for tubulin (scale bar, 50 μm).

(F) Sholl analysis was performed on WT and CPEB1 KO neurons cultured in phosphocreatine (n = 55 neurons from three mice). *p < 0.05, **p < 0.01 Student's t test, three replicates; the bars indicate SEM. See also Figure S3.

and ATP production lead to neurite stunting and perhaps loss of synaptic connections and inhibited synapse efficacy (Alarcon et al., 2004; Zearfoss et al., 2008).

DISCUSSION

Our studies show that in CPEB1 KO brain and neurons, deficient polyadenylation-induced translation of the complex I component NDUFV2 mRNA impairs mitochondrial ATP production, thus demonstrating a role for translational control in mouse neuronal bioenergetics. Why CPEB1 deficiency should inhibit ATP production only in the brain is unclear, but neurons as well as germ cells contain the greatest abundance of this protein, and thus NDUFV2 mRNA may not be regulated in other tissues because of a relative paucity of CPEB1. Complex I levels also differ among tissues, which have different energy requirements and sensitivities to defects in oxidative phosphorylation (Distelmaier et al., 2009; Koopman et al., 2010; Kunz, 2003). Perhaps the brain, which is the largest consumer of energy, may require CPEB1 to stimulate ATP generation in response to stress or synapse stimulation (Kann and Kovacs, 2007; Nicholls and Budd, 2000). It is important to note that steady-state levels of ATP are the result of both generation and consumption by cells. Although our report demonstrates that CPEB1 controls ATP

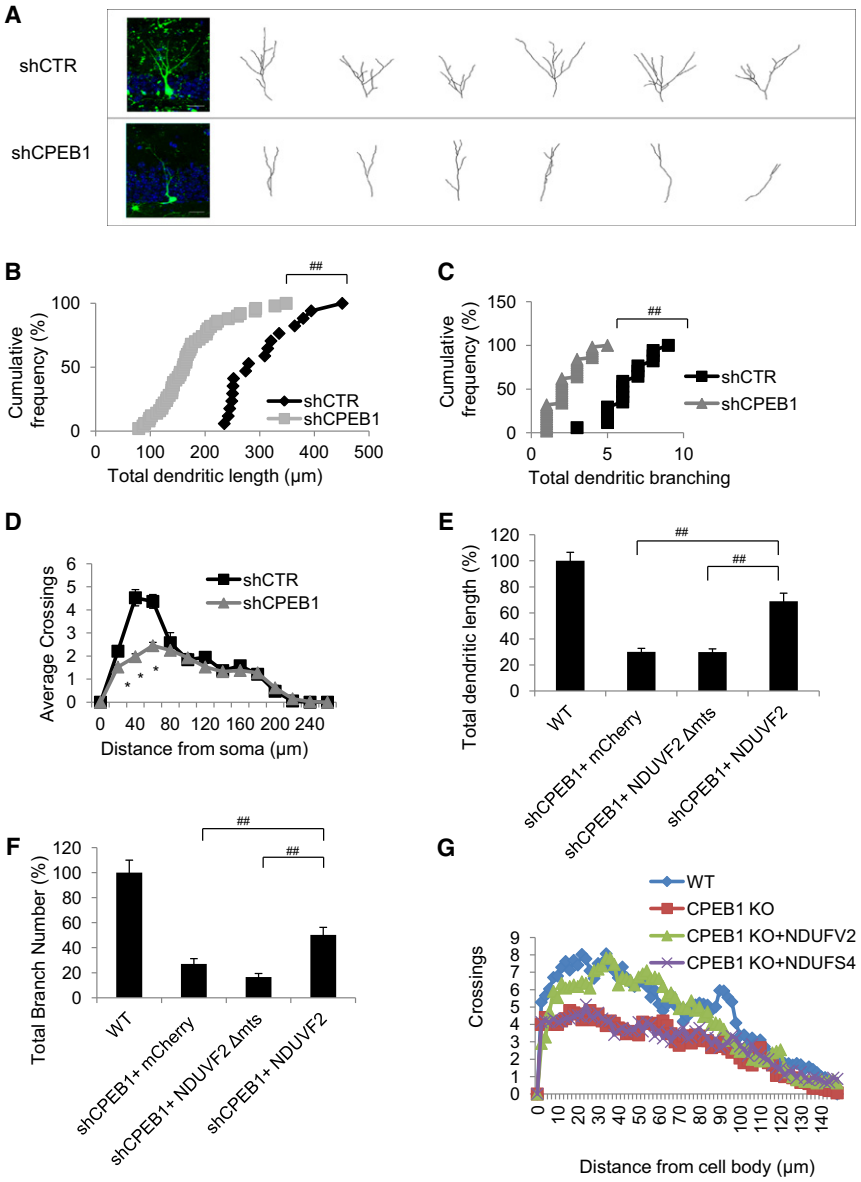

Figure 6. CPEB1 and NDUFV2 Control Dendrite Morphology In Vivo

(A) Three-dimensional (3D) confocal image reconstruction of dendrites from hippocampal dentate gyrus (DG) neurons that were stereotactically injected with retroviruses expressing GFP (control) or GFP and CPEB1 shRNA (14 dpi) (scale bar, 20 μm).

(B and C) Quantification of total dendritic length and branch number of dividing DG neurons.

(D) Sholl analysis of dendrite complexity of dividing DG neurons (14 dpi) (n = 4–6 animals). *p < 0.05, Student's t test, three replicates; ##p < 0.01, three replicates; the bars indicate SEM.

(E and F) Quantification of dendritic branch length and number following stereotactic DG injection of retroviruses expressing GFP and shRNA for CPEB1 plus either WT NDUFV2 or NDUFV2 that lacks its mitochondrial targeting sequence (MTS) (n = 12 animals).

(G) Sholl analysis of tubulin immunostained WT, CPEB1 KO, and CPEB1 KO hippocampal neurons infected in vitro with lentiviruses expressing NDUFV2 or as control NDUFS4.

The bars indicate SEM.

production by enhancing the translation of complex I protein NDUFV2 mRNA, we cannot rule out a possible effect of CPEB1 on ATP consumption as well. The control of ATP production by CPEB1 reported here contrasts to that which occurs during the Warburg effect. In transformed cells, aerobic glycolysis is due in part to aberrant splicing of pyruvate kinase; a predominant embryonic isoform, PKM2, is produced instead of the adult PKM1 form (David et al., 2010; Christofk et al., 2008). As a consequence, conversion of phosphoenolpyruvate (PEP) to pyruvate is reduced, limiting the amount of substrate for the tricarboxylic acid cycle (TCA) but stimulating the amount available for glycolysis (Chen et al., 2010).

Experiments using *Xenopus* oocytes demonstrated that Aurora A-catalyzed CPEB1 phosphoryation is necessary to stimulate very robust polyadenylation and translation (Mendez et al., 2000; Barnard et al., 2004; Kim and Richter, 2006; Groisman et al., 2002). In neurons, CPEB1 phosphorylation is also important for polyadenylation in response to synaptic activity (Udagawa et al., 2012). In these cases, CPEB1 responds to external signaling cues (hormones, synapse stimulation) to promote the expression of generally quiescent or at least inefficiently translated mRNAs. This CPEB1-mediated on-off switch for translation may not function in quite the same way for the polyadenylation of NDUFV2 mRNA observed here. That is, NDUFV2 would always be synthesized at some basal rate, but its expression might be turned up at times when ATP generation is particularly important, such as when neurites respond to guidance cues as they navigate to their final destinations. Thus, CPEB1 may act more like a rheostat to turn translation up or down, rather than a switch to turn translation on or off. The rheostat analogy may be similar to the case in MEFs or primary human fibroblasts where CPEB1 controls the expression of p53 in a relatively modest manner, although even a 50% change in p53 mRNA translation results in large alterations in cell physiology such as senescence bypass (Groisman et al., 2006; Burns and Richter, 2008; Groppo and Richter, 2011).

The importance of CPEB1 phosphorylation for neurite outgrowth was suggested by experiments of Bestman and Cline (2008, 2009), who electroporated a phosphorylation-defective "dominant-negative" CPEB1 into *Xenopus* tadpole optic tectal neurons and observed reduced dendrite branching as well as glutamatergic synaptic strength. These authors also showed that antisense morpholinos directed to CPEB1 mRNA, which would inhibit its translation, produced a similar effect. In this same vein, Lin et al. (2009) demonstrated that a dominant-negative CPEB1 introduced into *Xenopus* retinal ganglion neurons

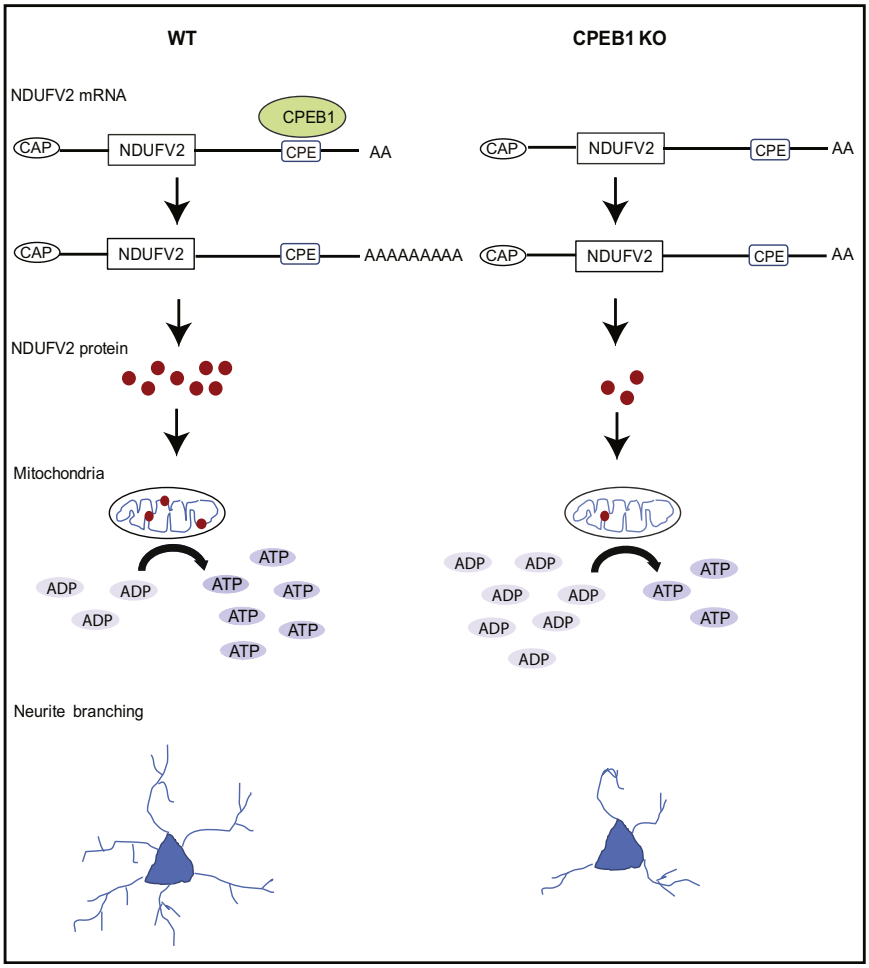

Figure 7. Model for CPEB1 Control of Energy Production in Neurons

CPEB1 associates with the 3′UTR CPEs of NDUFV2 mRNA in the cytoplasm of neurons. This interaction promotes poly(A) tail growth and translation of NDUFV2 mRNA, resulting in mitochondrial import of NDUFV2 protein, its incorporation into complex I, and elevated ATP production. ATP in turn is necessary for promoting neurite morphogenesis. In CPEB1 knockout (KO) neurons, a short poly(A) tail of NDUFV2 mRNA results in inefficient translation, which impedes complex I assembly and the generation of ATP. As a consequence, neurite outgrown is curtailed.

inhibited axon growth cones from properly extending axons. Although neither study identified the mRNA substrate(s) whose presumed reduced translation was responsible for the morphological defects in the neurons transduced with the dominant-negative CPEB1, our observations suggest that reduced ATP production caused by impaired NDUFV2 mRNA translation could be involved.

Because CPEB1 is transported to dendrites (Huang et al., 2003) where it mediates polyadenylation (Udagawa et al., 2012), we surmise that NDUFV2 mRNA polyadenylation and translation also occur in dendrites and probably cell bodies as well. Mitochondria are present at the base of dendritic spines where their ATP production is important for synapse function (Li et al., 2004). We envision that dendritic ATP is also important for neurite outgrowth and morphogenesis and that when neurons are CPEB1 deficient, reduced NDUFV2 mRNA translation and ATP production lead to neurite stunting and perhaps loss of synaptic connections and inhibited synapse efficacy (Alarcon et al., 2004; Zearfoss et al., 2008). Moreover, synapse stimulation induces not only CPEB1-dependent polyadenylation (Udagawa et al., 2012) but alterations in mitochondrial transport and localization as well (Chen and Chan, 2006). Thus, the CPEB1-mediated increase in mitochondrial activity could be an additional layer of stimulation-dependent regulation of ATP production.

Mitochondrial dysfunction is linked to several neurologic diseases including Parkinson's, Alzheimer's, and Huntington's diseases as well as amyotrophic lateral sclerosis (Lin and Beal 2006). Aberrant complex I in particular may be causative for Leigh disease, a neurodegenerative disorder (Loeffen et al., 1998), and a number of encephalopathies such as seizures, brainstem lesions, and dystonia (Distelmaier et al., 2009). These observations suggest that CPEB1 KO mice might also show signs of neurodegeneration elicited by impaired complex I activity. Gross examination of the CPEB1 KO mice shows no obvious signs of this malady; however, neurodegenerative diseases are progressive and may become obvious only in older mice. Consequently, further investigations are required to determine whether there is a neurodegenerative consequence to CPEB1 deficiency. In any case, CPEB1 KO mice display reduced complex I activity by only ~50%, which might be insufficient to cause obvious phenotypes such as those noted above. On the other hand, CPEB1 depletion reduces dendrite branching and development in the brain and alters synaptic efficacy. Moreover, impaired mitochondrial function inhibits dendrite spine density and synaptic plasticity (Li et al., 2004), suggesting that in the case of CPEB1 KO mouse, defective complex I could be responsible, at least in part, for a deficit in hippocampal long-term potentiation and hippocampus-dependent learning and memory (Alarcon et al., 2004; Berger-Sweeney et al., 2006).

EXPERIMENTAL PROCEDURES

Animals, Neuron Culture, and Isolation of Mitochondria

WT and CPEB1 C57BL/6 KO mice (Tay and Richter, 2001) were maintained in accordance with the Institutional Animal Care and Use Committee (IACUC) of the University of Massachusetts Medical School.

The culture of primary hippocampal and cortical neurons was performed as described (Huang and Richter, 2007) in neurobasal media (Invitrogen) containing B27 supplement (B27 media) and glutamine (1 μg/ml). Liver, muscle, and brain were dissected from 1-month-old female mice, washed, and homogenized in Krebs-Ringers bicarbonate buffer (125 mM NaCl, 1.4 mM KCl,

20 mM HEPES [pH 7.4], 5 mM $NaHCO_3$, 1.2 mM $MgSO_4$, 1.2 mM KH_2,PO_4, 1 mM $CaCl_2$) containing 1% BSA. Protein concentrations were determined using the BCA assay (Pierce). Mitochondria were isolated using a MITO-ISO1 kit (Sigma) and following the manufacturer's instructions.

ATP Determination

Fifty to 100 μg of brain lysate was used to measure ATP concentration using the CellTiter-Glo Luminescent Cell Viability kit (Promega) in a 96-well format. To measure ATP concentration in neurons, 60,000 cells were trypsinized from the dish, washed, and resuspended in 100 μl Krebs-Ringers bicarbonate buffer plus HEPES. The brain lysates and the cultured neuron lysates were aliquoted into 96-well plates and assayed according to manufacturer's instructions. To measure the recovery of ATP from brain lysates, known amounts of ATP (0.1, 1, 10, and 100 μM) were used to measure ATP bioluminescene using the CellTiter-Glo method as above in the presence or absence of WT or CPEB1 KO brain lysate. The recovery of ATP was calculated from these values.

Oxygen Consumption

To measure oxygen consumption in brain lysates, WT and CPEB1 KO mouse brains were washed and homogenized in 1 ml Krebs-Ringers bicarbonate buffer plus HEPES (125 mM NaCl, 1.4 mM KCl, 20 mM HEPES [pH 7.4], 5 mM $NaHCO_3$, 1.2 mM $MgSO_4$, 1.2 mM KH_2,PO_4, 1 mM $CaCl_2$) containing 1% BSA. Fifty to 100 μg of protein from each lysate was aliquoted into a BD Oxygen biosensor systems plate (BD Biosciences) in triplicate and assayed on a SAFIRE multimode microplate spectrophotometer at 1 min intervals for 120 min at an excitation wavelength of 485 nm and emission wavelength of 630 nm. To measure oxygen consumption in neurons and glia, 80,000 cells were washed, suspended in 200 μl Krebs-Ringers bicarbonate buffer, and aliquoted onto a BD Oxygen Biosensor systems plate in triplicate and assayed as described above. To measure nonmitochondrial oxygen consumption, the brain lysates and neurons were treated with 1 μM rotenone plus 10 μM antimycin.

Electron Transport Chain Enzyme Activities

Purified mitochondrial samples were freeze thawed three times before use in enzyme analysis to enable access of the substrate to the inner mitochondrial membrane. Enzyme activities were determined by adding exogenous substrates of the respective complexes and measuring the rate of conversion to product in isolated mitochondria. All analyses were performed on an Ultraspec 2000 UV/visible spectrophotometer (Pharmacia Biotech) in triplicate. Specific enzyme activities were calculated by subtracting the background activities using inhibitors to the complexes.

Measurement of Mitochondrial Respiration

Mitochondria were isolated from WT and CPEB1 KO mouse brain using differential centrifugation as described earlier. Oxygen consumption in the intact mitochondria was measured using Clark-type oxygen-sensitive electrode (YSI Incorporated). The assays were performed as described (Li and Graham, 2012).

Blue Native PAGE Electrophoresis

Mitochondria isolated from WT and CPEB1 KO mouse brain were resolved by blue native (BN)-PAGE as described (Wittig et al., 2006) and immunoblotted for mitochondrial proteins.

Translational Efficiency

DIV10 WT hippocampal neurons were cotransfected with 2 μg of pGL-3 and 2 μg of pRLTK-NDUFV2 3′UTR WT or 2 μg pRLTK-NDUFV2 3′UTR mutant. The transfected neurons were analyzed for Renilla luciferase and firefly luciferase using the dual luciferase assay system (Promega). The Renilla luciferase values were normalized to the firefly luciferase activity levels, which accounts for transfection efficiencies.

Metabolic Labeling

DIV6 cortical neurons were cultured in 100 mm plate for 30 min in methionine and cysteine-free media (Invitrogen); 60 μCi ^{35}S-methionine (ProMix, Amersham) was then added and the cells were cultured for 1 hr. The cells were lysed in 1 ml of 50 mM Tris-HCl [pH 8], 150 mM sodium chloride, 1% NP-40, 0.5% sodium deoxycholate, 0.1% SDS, and protease inhibitors. Lysates from WT and CPEB1 KO cells containing equivalent counts of radioactivity were then added to NDUFV2-protein A bead mixture, which was rotated overnight at 4°C. The beads were washed and analyzed by electrophoresis and phosphorimaging.

PAT Assay

For analysis of the poly(A) tail of the NDUFV2 mRNA, 10 μg of total RNA was extracted from brain using Trizol reagent (Invitrogen) and following the manufacturer's instructions. The RNA was annealed to oligo d(T) anchor (200 ng/μl; 5′-GCGAGCTCCGCGGCCGCGTTTTTTTTTTTT-3′) at 65°C for 5 min and then extended in a cDNA synthesis reaction using Superscript III (Invitrogen) at 50°C for 60 min according to manufacturer's instructions. cDNA template (1 μl) along with NDUFV2-specific primer and oligo d(T)anchor were used in a 25 μl PCR reaction with GoTaq (Invitrogen). PCR products were analyzed on 2.5% agarose gels.

Quantification of Dendritic Growth

Hippocampal neurons grown on coverslips were fixed in 4% paraformaldehyde in PBS containing 4% sucrose for 20 min at room temperature at various DIV. Coverslips were washed in PBS, permeabilized in 0.2% Triton X-100 for 7 min, blocked in 10% BSA solution, and immunostained with anti-alpha tubulin (Sigma, 1:1000 dilution). The neurons were then imaged using Nikon ECLIPSE E600 fluorescence microscope. The length of branches was calculated by tracing the dendrites in NeuronJ (plugin in ImageJ) software. The amount of branching was determined using the Sholl analysis plugin in ImageJ (NIH) software. Other neurons were supplemented daily with 1 mM phosphocreatine on DIV 2, 3, 4, and 5 before performing Sholl analysis on DIV 6.

Construction, Production, and Stereotactic Injection of Engineered Retroviruses

Engineered self-inactivating murine retroviruses were used to express GFP specifically in proliferating cells and their progeny. GFP expression was under the control of the eEF1α promoter, and the shRNA was coexpressed under the control of the human U6 promoter in the same vector. shRNA against mouse CPEB1 (position 1,466, gtcgtgtgactttcaataa) was cloned into a retroviral vector using a PCR SHAGing strategy. Adult (7–8 weeks old) female C57Bl/6 mice (Charles River) housed under standard conditions were anaesthetized (100 μg ketamine, 10 μg xylazine in 10 μl saline per gram), and retroviruses were stereotactically injected into the DGs as previously described (Ge et al., 2006). Mice were sacrificed at 14 days postinfection (dpi) for morphological analysis. Images were acquired on a Carl Zeiss LSM 710 confocal system and analyzed using Carl Zeiss Zen software. For analysis of the dendritic structure of neurons, the images were semiautomatically traced with NIH ImageJ using the NeuronJ plugin. Only granule cells with complete dendritic trees that were not overlapping with the other infected neurons were used for morphological characterization (neurons from four to six animals per condition were examined). The Sholl analysis for dendritic complexity was carried out by counting the number of dendrites that cross a series of concentric circles at 20 μm intervals from the soma. For ectopic expression of NDUVF2, a retroviral construct encoding for NDUVF2 fused to mCherry via a T2A linker was used (Szymczak et al., 2004). To determine whether NDUFV2 expression can rescue the dendritic branching dysfunction in the CPEB1-deficient neurons in vivo, mouse DGs were stereotactically injected with either of three groups of retroviruses: group 1 contained viruses expressing shRNA for CPEB1 and mcherry, group 2 contained viruses expressing shRNA for CPEB1 and WT NDUFV2, and group 3 contained viruses expressing shRNA for CPEB1 and NDUFV2 that lacked its MTS. The neurons were then analyzed as described above. Statistical significance ($p < 0.001$) was determined by one-way ANOVA with Newman-Keuls' post hoc test. All animal procedures and applicable regulations of animal welfare were in accordance with the IACUC guidelines and were approved by Singhealth IACUC in Singapore.

Statistical Analysis

Data were interpreted using Students t test, and the error bars indicate standard error of the mean (SEM). Statistical significance was determined by one-way ANOVA with Newman-Keuls' post hoc test.

SUPPLEMENTAL INFORMATION

Supplemental Information includes three figures, one table, Supplemental Experimental Procedures, and Supplemental References and can be found with this article online at http://dx.doi.org/10.1016/j.cmet.2012.11.002.

ACKNOWLEDGMENTS

We thank Nemisha Dawra and Maria Ivshina for mouse genotyping, Silvia Corvera for use of her clark type oxygen electrode, plate reader, and cytochrome *c* antibody, and members of the Richter lab for helpful discussions. T.U. was supported by fellowship from the FRAXA Foundation. This work was supported by grants from the NIH (AG30323, GM46779, and HD37267). Additional core support from the Diabetes Endocrinology Research Center (DK32520) is gratefully acknowledged.

Received: April 25, 2012
Revised: September 24, 2012
Accepted: November 5, 2012
Published: December 4, 2012

REFERENCES

Alarcon, J.M., Hodgman, R., Theis, M., Huang, Y.S., Kandel, E.R., and Richter, J.D. (2004). Selective modulation of some forms of schaffer collateral-CA1 synaptic plasticity in mice with a disruption of the CPEB-1 gene. Learn. Mem. *11*, 318–327.

Alexandrov, I.M., Ivshina, M., Jung, D.Y., Friedline, R., Ko, H.J., Xu, M., O'Sullivan-Murphy, B., Bortell, R., Huang, Y.T., Urano, F., et al. (2012). Cytoplasmic Polyadenylation element binding protein deficiency stimulates PTEN and Stat3 mRNA translation and induces hepatic insulin resistance. PLoS Genet. *8*, e1002457. http://dx.doi.org/10.1371/journal.pgen.1002457.

Barnard, D.C., Ryan, K., Manley, J.L., and Richter, J.D. (2004). Symplekin and xGLD-2 are required for CPEB-mediated cytoplasmic polyadenylation. Cell *119*, 641–651.

Berger-Sweeney, J., Zearfoss, N.R., and Richter, J.D. (2006). Reduced extinction of hippocampal-dependent memories in CPEB knockout mice. Learn. Mem. *13*, 4–7.

Bestman, J.E., and Cline, H.T. (2008). The RNA binding protein CPEB regulates dendrite morphogenesis and neuronal circuit assembly in vivo. Proc. Natl. Acad. Sci. USA *105*, 20494–20499.

Bestman, J.E., and Cline, H.T. (2009). The relationship between dendritic branch dynamics and CPEB-labeled RNP granules captured in vivo. Front. Neural. Circuits *3*, 10. http://dx.doi.org/10.3389/neuro.04.010.2009.

Burns, D.M., and Richter, J.D. (2008). CPEB regulation of human cellular senescence, energy metabolism, and p53 mRNA translation. Genes Dev. *22*, 3449–3460.

Cao, Q., Kim, J.H., and Richter, J.D. (2006). CDK1 and calcineurin regulate Maskin association with eIF4E and translational control of cell cycle progression. Nat. Struct. Mol. Biol. *13*, 1128–1134.

Chen, H., and Chan, D.C. (2006). Critical dependence of neurons on mitochondrial dynamics. Curr. Opin. Cell Biol. *18*, 453–459.

Chen, P.J., and Huang, Y.S. (2011). CPEB2-eEF2 interaction impedes HIF-1α RNA translation. EMBO J. *31*, 959–971.

Chen, M., Zhang, J., and Manley, J.L. (2010). Turning on a fuel switch of cancer: hnRNP proteins regulate alternative splicing of pyruvate kinase mRNA. Cancer Res. *70*, 8977–8980.

Christofk, H.R., Vander Heiden, M.G., Harris, M.H., Ramanathan, A., Gerszten, R.E., Wei, R., Fleming, M.D., Schreiber, S.L., and Cantley, L.C. (2008). The M2 splice isoform of pyruvate kinase is important for cancer metabolism and tumour growth. Nature *452*, 230–233.

Dang, C.V. (2012). Links between metabolism and cancer. Genes Dev. *26*, 877–890.

David, C.J., Chen, M., Assanah, M., Canoll, P., and Manley, J.L. (2010). HnRNP proteins controlled by c-Myc deregulate pyruvate kinase mRNA splicing in cancer. Nature *463*, 364–368.

Distelmaier, F., Koopman, W.J., van den Heuvel, L.P., Rodenburg, R.J., Mayatepek, E., Willems, P.H., and Smeitink, J.A. (2009). Mitochondrial complex I deficiency: from organelle dysfunction to clinical disease. Brain *132*, 833–842.

Fox, C.A., Sheets, M.D., and Wickens, M.P. (1989). Poly(A) addition during maturation of frog oocytes: distinct nuclear and cytoplasmic activities and regulation by the sequence UUUUUAU. Genes Dev. *3*, 2151–2162.

Ge, S., Goh, E.L., Sailor, K.A., Kitabatake, Y., Ming, G.L., and Song, H. (2006). GABA regulates synaptic integration of newly generated neurons in the adult brain. Nature *439*, 589–593.

Groisman, I., Jung, M.Y., Sarkissian, M., Cao, Q., and Richter, J.D. (2002). Translational control of the embryonic cell cycle. Cell *109*, 473–483.

Groisman, I., Ivshina, M., Marin, V., Kennedy, N.J., Davis, R.J., and Richter, J.D. (2006). Control of cellular senescence by CPEB. Genes Dev. *20*, 2701–2712.

Groppo, R., and Richter, J.D. (2011). CPEB control of NF-kappaB nuclear localization and interleukin-6 production mediates cellular senescence. Mol. Cell. Biol. *31*, 2707–2714.

Huang, Y.S., and Richter, J.D. (2007). Analysis of mRNA translation in cultured hippocampal neurons. Methods Enzymol. *431*, 143–162.

Huang, Y.S., Carson, J.H., Barbarese, E., and Richter, J.D. (2003). Facilitation of dendritic mRNA transport by CPEB. Genes Dev. *17*, 638–653.

Huang, Y.S., Kan, M.C., Lin, C.L., and Richter, J.D. (2006). CPEB3 and CPEB4 in neurons: analysis of RNA-binding specificity and translational control of AMPA receptor GluR2 mRNA. EMBO J. *25*, 4865–4876.

Kann, O., and Kovacs, R. (2007). Mitochondria and neuronal activity. Am. J. Physiol. Cell Physiol. *292*, C641–C657.

Kim, J.H., and Richter, J.D. (2006). Opposing polymerase-deadenylase activities regulate cytoplasmic polyadenylation. Mol. Cell *24*, 173–183.

Kim, J.H., and Richter, J.D. (2007). RINGO/cdk1 and CPEB mediate poly(A) tail stabilization and translational regulation by ePAB. Genes Dev. *21*, 2571–2579.

Koc, E.C., and Koc, H. (2012). Regulation of mammalian mitochondrial translation by 3 post-translational modifications. Biochim. Biophys. Acta *1819*, 1055–1066.

Koopman, W.J., Nijtmans, L.G., Dieteren, C.E., Roestenberg, P., Valsecchi, F., Smeitink, J.A., and Willems, P.H. (2010). Mammalian mitochondrial complex I: biogenesis, regulation, and reactive oxygen species generation. Antioxid. Redox Signal. *12*, 1431–1470.

Kunz, W.S. (2003). Different metabolic properties of mitochondrial oxidative phosphorylation in different cell types—important implications for mitochondrial cytopathies. Exp. Physiol. *88*, 149–154.

Levine, A.J., and Puzio-Kuter, A.M. (2010). The control of the metabolic switch in cancers by oncogenes and tumor suppressor genes. Science *330*, 1340–1344.

Li, Z., and Graham, B.H. (2012). Measurement of mitochondrial oxygen consumption using a Clark electrode. Methods Mol. Biol. *837*, 63–72.

Li, Z., Okamoto, K., Hayashi, Y., and Sheng, M. (2004). The importance of dendritic mitochondria in the morphogenesis and plasticity of spines and synapses. Cell *119*, 873–887.

Lin, M.T., and Beal, M.F. (2006). Mitochondrial dysfunction and oxidative stress in neurodegenerative diseases. Nature *443*, 787–795.

Lin, J., Handschin, C., and Spiegelman, B.M. (2005). Metabolic control through the PGC1 family of transcription coactivators. Cell Metab. *1*, 361–370.

Lin, A.C., Tan, C.T., Lin, C.L., Strochlic, L., Huang, Y., Richter, J.D., and Holt, C.E. (2009). Cytoplasmic polyadenylation and cytoplasmic polyadenylation element-dependent mRNA regulation are involved in *Xenopus* retinal axon development. Neural Dev. *4*, 8. http://dx.doi.org/10.1186/1749-8104-4-8.

Loeffen, J., Smeitink, J., Triepels, R., Smeets, R., Schuelke, M., Sengers, R., Trijbels, F., Hamel, B., Mullaart, R., and van den Heuvel, L. (1998). The first

nuclear-encoded complex I mutation in a patient with Leigh syndrome. Am. J. Hum. Genet. *63*, 1598–1608.

Mendez, R., and Richter, J.D. (2001). Translational control by CPEB: a means to the end. Nat. Rev. Mol. Cell Biol. *2*, 521–529.

Mendez, R., Hake, L.E., Andresson, T., Littlepage, L.E., Ruderman, J.V., and Richter, J.D. (2000). Phosphorylation of CPE binding factor by Eg2 regulates translation of c-mos mRNA. Nature *404*, 302–307.

Nicholls, D.G., and Budd, S.L. (2000). Mitochondria and neuronal survival. Physiol. Rev. *80*, 315–360.

Novoa, I., Gallego, J., Ferreira, P.G., and Mendez, R. (2010). Mitotic cell-cycle progression is regulated by CPEB1 and CPEB4-dependent translational control. Nat. Cell Biol. *12*, 447–456.

Pagliarini, D.J., Calvo, S.E., Chang, B., Sheth, S.A., Vafai, S.B., Ong, S.E., Walford, G.A., Sugiana, C., Boneh, A., Chen, W.K., et al. (2008). A mitochondrial protein compendium elucidates complex I disease biology. Cell *134*, 112–123.

Richter, J.D. (2007). CPEB: a life in translation. Trends Biochem. Sci. *32*, 279–285.

Scarpulla, R.C. (2008). Nuclear control of respiratory chain expression by nuclear respiratory factors and PGC-1-related coactivator. Ann. N Y Acad. Sci. *1147*, 321–334.

Shoubridge, E.A. (2012). Supersizing the mitochondrial respiratory chain. Cell Metab. *15*, 271–272.

Szymczak, A.L., Workman, C.J., Wang, Y., Vignali, K.M., Dilioglou, S., Vanin, E.F., and Vignali, D.A. (2004). Correction of multi-gene deficiency in vivo using a single 'self-cleaving' 2A peptide-based retroviral vector. Nat. Biotechnol. *22*, 589–594.

Tay, J., and Richter, J.D. (2001). Germ cell differentiation and synaptonemal complex formation are disrupted in CPEB knockout mice. Dev. Cell *1*, 201–213.

Udagawa, T., Swanger, S.A., Takeuchi, K., Kim, J.H., Nalavadi, V., Shin, J., Lorenz, L.J., Zukin, R.S., Bassell, G.J., and Richter, J.D. (2012). Bidirectional control of mRNA translation and synaptic plasticity by the cytoplasmic polyadenylation complex. Mol. Cell *47*, 253–266.

Vander Heiden, M.G., Cantley, L.C., and Thompson, C.B. (2009). Understanding the Warburg effect: the metabolic requirements of cell proliferation. Science *324*, 1029–1033.

Wang, C.F., and Huang, Y.S. (2012). Calpain 2 activated through N-methyl-D-aspartic acid receptor signaling cleaves CPEB3 and abrogates CPEB3-repressed translation in neurons. Mol. Cell. Biol. *32*, 3321–3332.

Wittig, I., Braun, H.P., and Schagger, H. (2006). Blue native PAGE. Nat. Protoc. *1*, 418–428.

Zearfoss, N.R., Alarcon, J.M., Trifilieff, P., Kandel, E., and Richter, J.D. (2008). A molecular circuit composed of CPEB-1 and c-Jun controls growth hormone-mediated synaptic plasticity in the mouse hippocampus. J. Neurosci. *28*, 8502–8509.